



HAL
open science

Cholesteric liquid crystalline materials reflecting more than 50% of unpolarized incident light intensity

Michel Mitov, Nathalie Dessaud

► **To cite this version:**

Michel Mitov, Nathalie Dessaud. Cholesteric liquid crystalline materials reflecting more than 50% of unpolarized incident light intensity. *Liquid Crystals*, 2007, 34 (2), pp.183-193. 10.1080/02678290601116175 . hal-03588361

HAL Id: hal-03588361

<https://hal.science/hal-03588361>

Submitted on 4 Mar 2022

HAL is a multi-disciplinary open access archive for the deposit and dissemination of scientific research documents, whether they are published or not. The documents may come from teaching and research institutions in France or abroad, or from public or private research centers.

L'archive ouverte pluridisciplinaire **HAL**, est destinée au dépôt et à la diffusion de documents scientifiques de niveau recherche, publiés ou non, émanant des établissements d'enseignement et de recherche français ou étrangers, des laboratoires publics ou privés.

Cholesteric liquid crystalline materials reflecting more than 50% of unpolarized incident light intensity

Michel Mitov* and Nathalie Dessaud†

Centre d'Elaboration de Matériaux et d'Etudes Structurales, CEMES, CNRS,

BP 94347, 29 rue Jeanne-Marvig, F-31055 Toulouse cedex 4, France

Article history: Received 25 May 2006; in final form 30 August 2006; accepted 6 September 2006.

<https://doi.org/10.1080/02678290601116175>

* Author for correspondence: mitov@cemes.fr

† Now at: Philips Research, Display Applications and Technologies, Postbox MS 41, Building 34 (WB), High Tech Campus 34 , 5656 AE Eindhoven, The Netherlands.

Cholesteric liquid crystals (CLC) selectively reflect the light when the wavelength matches the helical pitch. The reflectance is limited to 50% of ambient, unpolarized, light because circularly polarized light of the same handedness than the helix is reflected. Here the elaboration procedure and the properties of a CLC gel whose the optical characteristics go beyond the 50% reflectance limit are reported. Photopolymerizable monomers are introduced in the volume of a CLC exhibiting a thermally-induced helicity inversion and the blend is then cured with UV-light when the helix is right-handed. The reflectance exceeds 50% when measured at the temperature assigned at a cholesteric helix with the same pitch but a left-handed sense before reaction. The reflection properties are investigated in the infrared region. From scanning electron microscopy investigations, it is shown that the organization of the mesophase is transferred onto the structure of the network. The gel structure is discussed as consisting of a polymer network with a helical structure containing two populations of low molar mass LC molecules. Each of them was characterized by a band of circularly polarized light which is selectively reflected. The monitoring of the optical response with the temperature offers the opportunity to discriminate the respective contributions of bound and free fraction of LC molecules to the reflectance and to give evidence of the progressive increase of the reflected flux when the temperature decreases from the curing temperature. Novel opportunities to modulate the reflection over the whole light flux range are offered. Potential applications are related to the light management for smart windows or reflective polarizer-free displays with a larger scale of reflectivity levels.

1. Introduction

1.1. Selective light reflection of cholesteric liquid crystals

A cholesteric liquid crystal (CLC), or chiral nematic LC, exhibits unique optical properties [1]. When the incident light propagates essentially along the helical axis (*i.e.* when the CLC slab exhibits a planar Grandjean texture), a selective reflection occurs if the wavelength λ_0 is of the order of the pitch p of the helix such that:

$$\lambda_0 = n p \cos\theta,$$

where n is the average refractive index, $(n_{//} + n_{\perp})/2$ ($n_{//}$ and n_{\perp} are locally parallel and perpendicular to the director), and θ is the angle between the propagation direction and the helix axis. The reflection occurs within a bandwidth $\Delta\lambda = \Delta n p \cos\theta$, where $\Delta n = n_{//} - n_{\perp}$; outside this band, a CLC affects neither the amplitude nor the state of polarization of the transmitted light. The reflected light is also circularly polarized with the same handedness as the incident light, which is the exact opposite of a normal dielectric mirror that changes the handedness. For example, right-handed circularly polarized incident light is reflected by a right-handed helix and, in contrast, if left-handed circularly polarized, the incident light is transmitted without significant loss through the medium. Consequently, as only circularly polarized light with one handedness is reflected, the maximum reflection of ambient – unpolarized – light from a CLC is never greater than 50%.

1.2. The scope of this paper

The objective of the work is to show that exceeding the theoretical limit of 50% for the reflected light may be reached by polymerizing under peculiar conditions a small quantity of mesomorphic photoreactive monomers in the volume of a low molar mass CLC. This result was briefly reported by us in a previous letter intended for a broad readership [2]. The scope of the present paper is to give a detailed description of the preparation of the CLC films giving rise to an unusual flux of reflected light, their polymorphism and their optical behaviour with the temperature before and after curing, and to widen the discussion.

1.3. Key idea of the elaboration path

CLCs exhibiting the phenomenon of thermally-induced helicity inversion are taken into consideration. Such a phenomenon occurs when the handedness of the helical structure is changed with the temperature, leading to a nematic state (infinite-pitch CLC) at the inversion temperature [3, 4]. Due to the temperature-sensitivity of the chirality, helix inversion compounds are excellent systems to probe the microscopic origin of the chirality in LC phases. Two general explanations for the helix inversion behaviour have been suggested. In one, the statistical distribution of the many molecular conformations shifts with changing the temperature [5, 6]. In the other, the competition between the different temperature dependences and opposite chiralities of multiple chiral centers causes the helix inversion [7, 8]. Experimental support for the first

explanation comes from nematic systems with chiral dopants [9, 10], whereas results verifying the second explanation use diastereomeric LC compounds [11, 12].

Photopolymerizable and crosslinkable nematic monomers are here introduced in the volume of a CLC exhibiting a thermally-induced helicity inversion and the blend is cured with UV-light when the helix is right-handed. Due to memory effects brought by the polymer network, it is expected that the reflectance may exceed 50% of the unpolarized incident light when measured at the temperature assigned at a cholesteric helix with the same pitch but a left-handed sense before reaction. Since CLCs are used as tunable bandpass filters, reflectors or polarizers and temperature or pressure sensors [13], novel opportunities to modulate the reflection over the whole light flux range may be offered.

2. Experimental details

2.1. Polymorphism of the LC blend.- It consists of the nematic LC BL006 (from Merck Ltd.; used at 71.2 wt.%), the RM257 bifunctional photoreactive nematic compound (diacrylate from Merck Ltd.; used at 3.8 wt.%) and, to induce the helicity inversion, the chiral dopant DL6 which is a propanediol derivative (Figure 1), used here at 25 wt.% and called 1b in reference [14] in which the synthesis details are given.

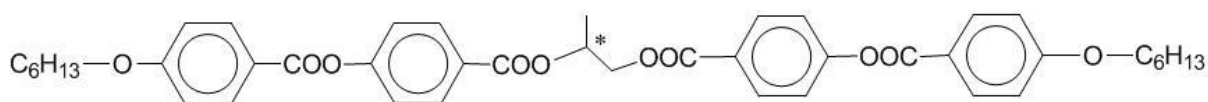


Figure 1. Structure of the mesogenic ester of (S)-1,2-propanediol used as chiral compound inducing the cholesteric phase with a thermally-induced inversion of the helicity sense. See Ref. 14 for the synthesis details.

The blend is introduced by capillarity at 90°C into a glass sandwich-cell. The helicity sense of the blend as a function of temperature is determined as follows. A series of home-made CLC polarizers is used; their pass-band is tuned with the reflection wavelength of the blend at each temperature (see below for the exact nature of the polarizers). For the determination of the helicity sense of the cholesteric sample, a given circular polarizer was placed between the light beam and the investigation cell. As an example, if the polarizer is right circular, the light transmitted through the cell is then close to 100 (0) % of the light transmitted by the polarizer if the helicity sense of the cell is left (right).

The phases were identified by using polarizing microscopy. The cholesteric to isotropic phase transition occurred at 114°C. The sample showed a helicity inversion at $T_c = 92^\circ\text{C}$ and exhibited a planar nematic texture with four extinction positions between crossed polarizers. The transmittance spectra were investigated by IR spectroscopy between 2.50 and 4.50 μm which will be the investigation range of the present study. The variation of reflection wavelength with the temperature is shown in Figure 2; our own convention is to report negative (positive) wavelength values when the helix is left- (right-) handed.

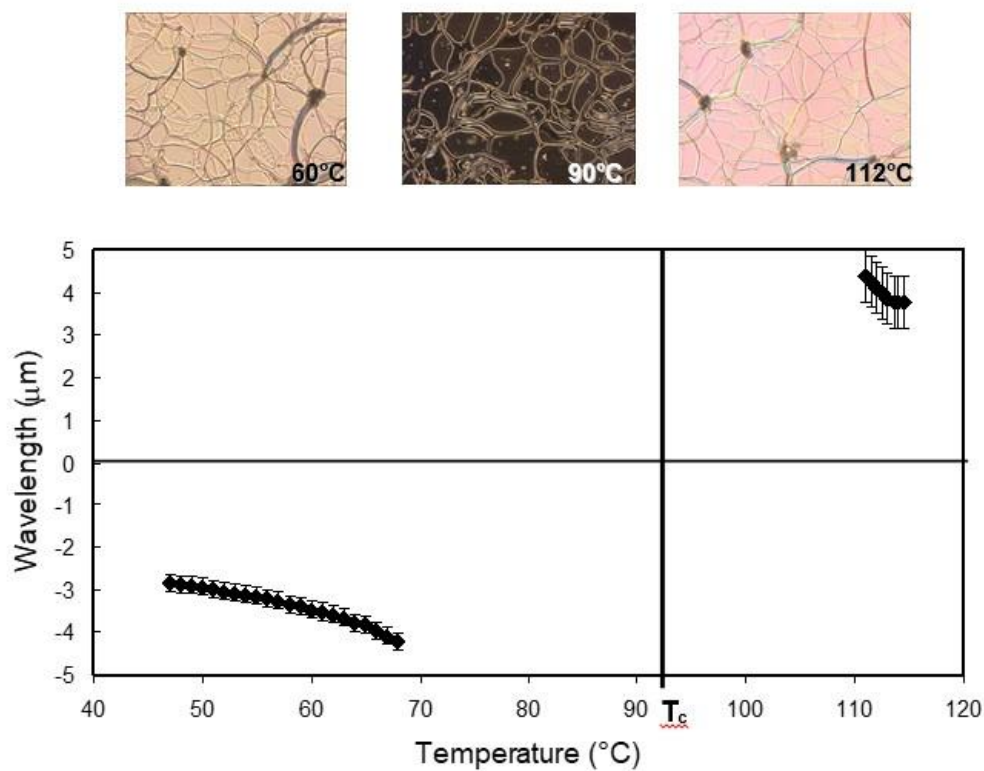


Figure 2. Variation of the reflection wavelength of the cholesteric mixture with the temperature. Inserted: three typical textures as observed by polarized optical microscopy (transmission mode).

Below T_c , the helix is left-handed and the reflection wavelength changes inside the investigated range from 2.8 to 4.2 μm when the temperature increases. Above T_c , the helix is right-handed and the wavelength changes from 4.4 to 3.8 μm inside the investigated range. Three typical optical textures (transmission mode) are inserted in Figure 2. They correspond to cholesteric planar textures with oily streaks, below and above the inversion temperature, at 60 and 112°C – which are two operating

temperatures in the forthcoming procedure – and to a homeotropic (unwound cholesteric) state at the very close neighbouring of the inversion temperature.

2.2. Experimental cells.- We used 50 ± 10 μm thick indium tin oxide (ITO)-coated glass sandwich-cells (from EHC Co. Ltd) with a planar alignment due to polyimide layers which were uniaxially rubbed and assembled at an 180°C angle with respect to each rubbing direction. Our purpose was to use standard calibrated glass cells but not especially ITO-coated glass for the study which is reported here. However, because we plan electro-optical measurements in the future, we decided to choose these cells at the beginning of our research programme for methodology purposes.

2.3. IR spectroscopy.- Transmittance spectra were investigated by using a Perkin Elmer IR spectrophotometer, coupled with a Mettler hot stage, with a compartment in which different narrow band circular polarizers can be positioned. The baseline was done when the cell was placed at the helix inversion temperature $T_c = 92^\circ\text{C}$ and when a cell filled with 100% of the CLC BL094 (from Merck Ltd.) is introduced in the unpolarized light beam; the reason of the presence of BL094 will be understood from the details about the nature of the polarizers given in the following paragraph. These baseline conditions allow to remove from the transmitted signal the signature of the chemical bonds absorption and losses in diffusion, to concentrate the investigation on the Bragg reflection phenomenon. All spectra were normalized to have an amount of light transmitted of 100% at $2.5\mu\text{m}$, *i.e.* for a wavelength far from the reflection band. On the spectra, the shadowed areas mark the chemical absorption bands.

2.4. Nature of the polarizers for spectroscopy.- Home-made circular polarizers were used when investigations with polarized incident light were required. For this purpose, blends of BL094 and BL095 CLCs (from Merck Ltd.) were made. These compounds are enantiomers which selectively reflect light at 548 nm at room temperature. BL094 (BL095) is right- (left-) handed. A nematic structure is obtained when the compounds are blended in the same proportions (racemic mixture). Circular polarizers with a tunable-wavelength reflection band and a helix either right- or left-handed are fabricated by varying the relative concentration of one enantiomer with the other one. As a consequence, the polarizers are also reflectors: a left- (right-) handed helix gives rise to a right (left) circular polarizer. A 25 ± 5 μm thick cell was then filled with the blend corresponding to a pass-band superimposed with the investigated reflection band of the sample. For example, in the case of data in Figure 5 (which reveal the phenomenon), the left (right) circular polarizer corresponds to a BL094 : BL095 wt.% ratio equal to 57 ± 1 : 43 ± 1 (43 ± 1 : 57 ± 1). In the case of data in Figure 3, due to the fact that the helical pitch of the blend slightly decreases as a consequence of the photoreaction (see sub-section 3.2 and Figure 4), the pass-band for the polarizers which are used for the characterization of optical properties before UV-curing was different, which means that the ratio has to be changed; in that case, the left (right) circular polarizer corresponds to a BL094 : BL095 wt.% ratio equal to 56 ± 1 : 44 ± 1 (44 ± 1 : 56 ± 1).

2.5. Observations by Scanning Electron Microscopy (SEM).- Conventional preparation techniques consist of breaking or cutting the sample and removal of the LC by solvent to expose the polymer network. One of the glass plates was removed when the cell was at the liquid nitrogen temperature. Then the semi-free sample is immersed

for 2 hours at room temperature in a cyanobiphenyl LC in isotropic phase (CB15 from Merck Ltd.). This intermediary step – before the immersion in a non-mesogenic isotropic solvent – facilitates the LC dissociation from the network (it means that a LC in isotropic phase has to be dissolved in an isotropic solvent). Finally, the cell was immersed in cyclohexane for three days to leave bare the network. Samples were coated with a platinum film and observed using a Jeol JSM 6700F field-emission SEM.

3. Results

3.1. Optical behaviour before curing

The cell exhibits a very well aligned reflective (planar) texture, due to a confinement ratio (thickness : pitch ratio) equal to 18 ± 6 , fitting for clear-cut reflection peaks. Figure 3 shows the transmittance spectra of the cell for different polarization cases of incident light at 112°C , when the reflection wavelength is equal to $4.2 \mu\text{m}$.

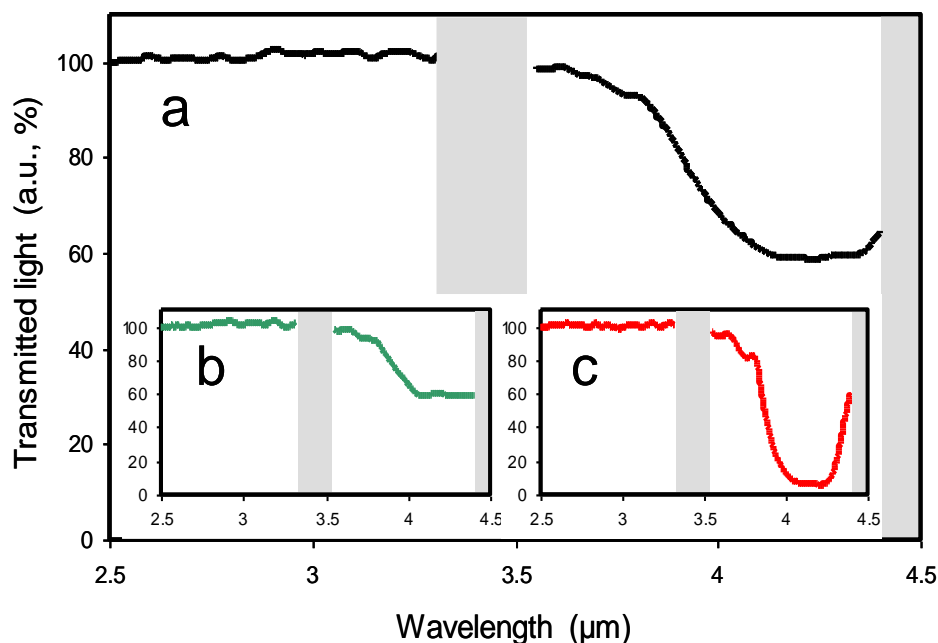


Figure 3. Normalized transmission spectra at 112°C before UV-reaction, when the incident light is unpolarized (a) or after the introduction in the light beam path of a left (b) or right (c) circular polarizer. (The shadowed areas mark the chemical absorption bands).

Due to the fact that the helix is right-handed, the maximum reflection intensity is close to 40% – at least less than 50% – when the incident light beam is unpolarized (Figure 3.a), or after the introduction of a left-circular polarizer (Figure 3.b) because this polarizer is also a reflector (it reflects the right-circularly polarized component). It is close to 90% after the introduction of a right-circular polarizer (Figure 3.c) as both the left- and right-circularly polarized components are reflected respectively by the polarizer and the cell. The expected behaviours are thus confirmed.

3.2. Optical behaviour after curing: towards an unusually large level of reflected light intensity

The cell is cured with UV-light (with the wavelength of maximum intensity of 0.1 mW/cm² centred around 365 nm) at 112°C for 4 hours, while the cholesteric helix is right-handed. When the reflectance properties are investigated at 112°C, the reflection wavelength is shifted from 4.2 to 3.8 μm (Figure 4) as a result of polymer network formation in the LC matrix.

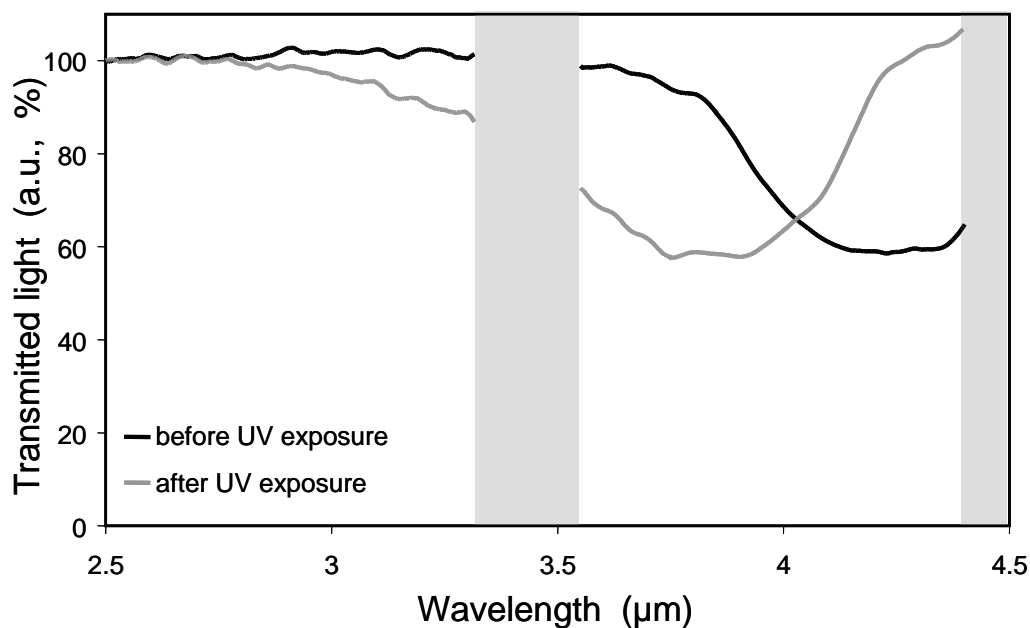


Figure 4. Normalized transmission spectra at 112°C before and after UV-reaction, when the incident light is unpolarized. (The shadowed areas mark the chemical absorption bands).

The helical pitch of the blend is believed to slightly decrease in relation with the volume shrinkage coming from the reaction of polymerization and crosslinking. Such a behaviour had previously been observed during the formation of three-dimensionally ordered polymer networks with a helical structure [15].

Figure 5 shows the transmission spectra of the same cell at 60°C, after cooling. At 60°C and before gelation, the selective reflection was close to 3.8 μm and associated to a left-handed helix. A chemical absorption band approaches close to 4.5 μm, as a result of which the normalized transmitted intensity diverges above 100%.

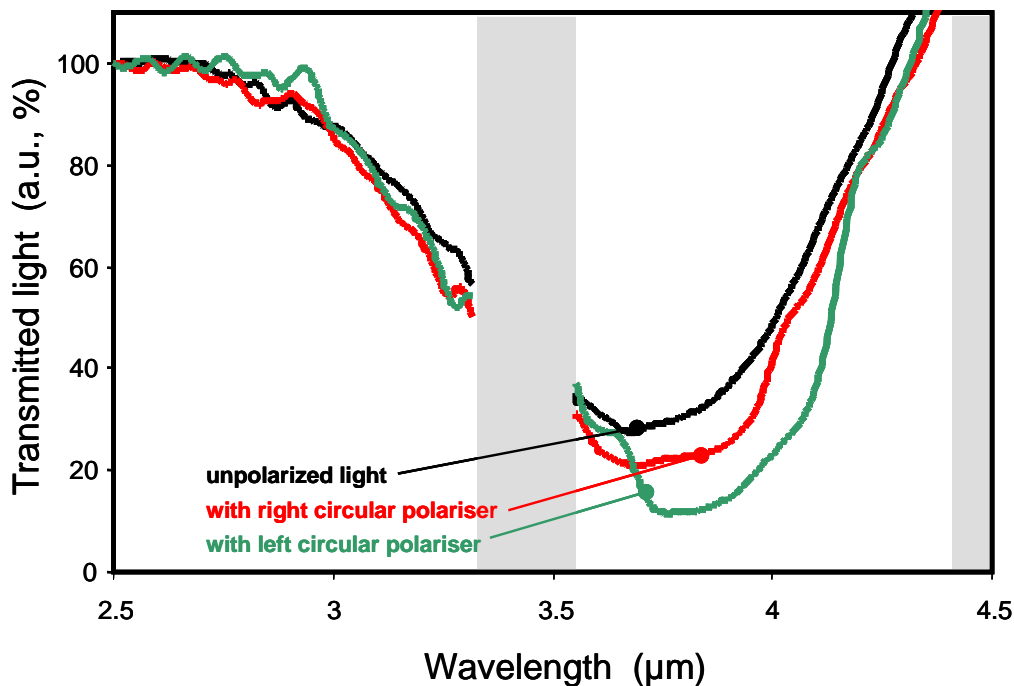


Figure 5. Normalized transmission spectra at 60°C, after UV-reaction at 112°C, when the incident light is unpolarized or a left or a right circular polarizer is introduced in the light beam path. (The shadowed areas mark the chemical absorption bands. A chemical absorption band approaches close to 4.5 μm , as a result of which the normalized transmitted intensity diverges above 100%).

From Figure 5, using unpolarized light or introducing a right or left circular polarizer in the beam path, we deduce that the reflected intensities are respectively equal to 72, 78 and 88%. These quantities are reduced to the flux of the unpolarized light source at 2.5 μm (see the section 2.3 about the normalization conditions). Now, we can also consider as the reference flux the light being incident on the cell – *i.e.* after having crossed a circular polarizer (reflecting 50% of the source because the polarizers are here also reflectors); therefore we deduce that the reflected intensities are equal to: 76% (*i.e.*:

$(88 - 50) \times 2$) of a left circularly polarized incident light and to 56% (*i.e.*: $(78 - 50) \times 2$) of a right one. In conclusion, whatever the polarization of the incident light is, the reflectance of the cholesteric film goes over 50%: the usual polarization-selectivity rule is here no more valid.

3.3. Morphology of the polymer network

The polymer morphology, as investigated by SEM, exhibits smooth polymer strands (Figure 6), like the signature of a good solubility of the monomers within the LC; the behaviour may be understood in the context of the Flory-Huggins model of polymer solubility [16], which is the primary factor determining the network morphology.

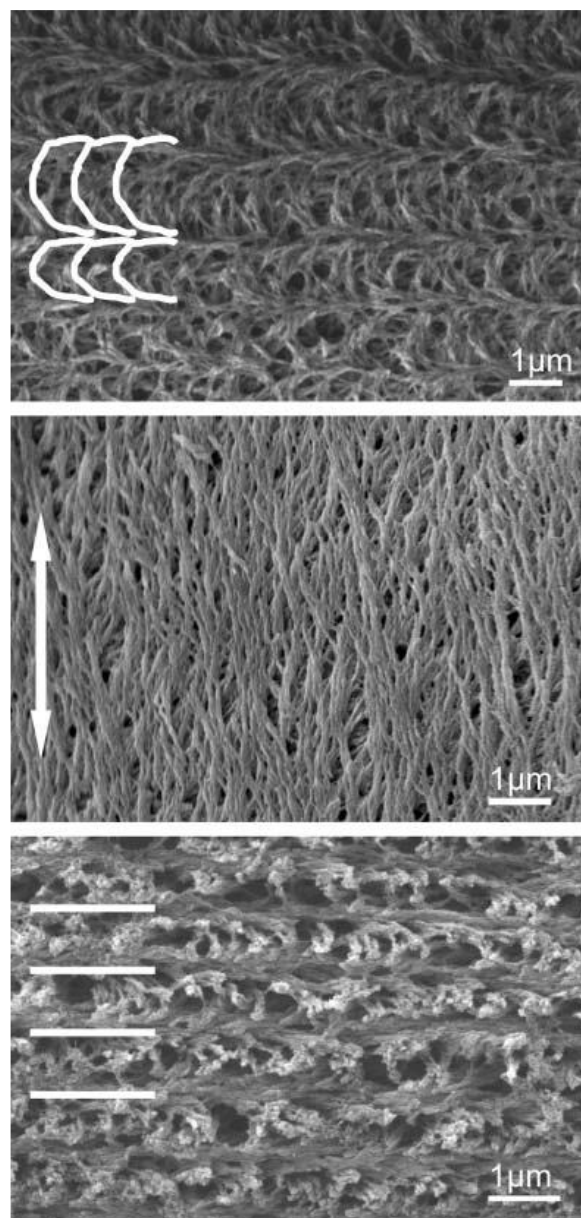


Figure 6. Scanning electron microscopy images of the polymer network formed in the cholesteric phase. The helical structure has been transferred onto the polymer morphology. The polymer fibrils draw stacked rows of parallel arcs which appear when the cut direction is oblique to the helical axis (a); these arcs are enhanced in white on the left part of the picture. The fibres are viewed as parallel together in a cut direction parallel to the surfaces (b); the double-arrow represents the mean orientation of the fibres: this micrograph shows the locally transferred nematic order. A layered system of

fibres appears when the polymer network is cut and viewed in a direction strictly perpendicular to the surfaces (c); white bars localize the position of a few layers.

Figure 6.a displays polymer fibrils as stacked rows of parallel arcs which appear when the cut direction is oblique to the helical axis. Such arced patterns were visible in thin sections of biological materials: crustacean integuments [17], dermal plates of fishes [18], insect cuticles [17, 19, 20], collageneous matrices of bone tissue [21], plant cell walls [22] and chromatin organizations for DNA [23]; they have also been observed in man-made polymer-stabilized CLCs [24].

The arced patterns found in these widely differing systems have a common physical origin: a twisted plywood model to account for such an architecture was proposed by Yves Bouligand [25]. Here, and by analogy, the architecture is as follows. The material appears to be made of superimposed lamellae of polymer fibres, which are parallel to the glass plate (Figure 6.b). We define the plane of this latter as being horizontal. Each lamella contains parallel arcs when observed in oblique sections (Figure 6.a). In contrast, in vertical section – that is, normal to the glass plate – the arcs disappear but the stratification persists (Figure 6.c). As the plane of the section approaches the plane of the layers, the arcs appear larger. In summary, and as sketched in Figure 7, the present system is made of polymer fibrils that are horizontal, parallel within any given horizontal plane, and with a direction that rotates continuously as one proceeds through successive levels of the bulk polymer. This is exactly the geometry of the cholesteric structure.

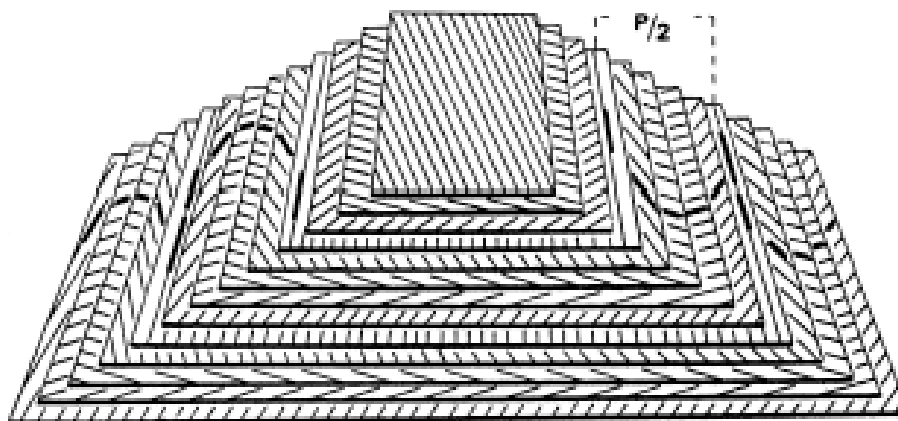


Figure 7. Three-dimensional model of the cholesteric organization of the polymer network. Superimposed cards represent equidistant and parallel planes. On each card the polymer fibrils are represented as parallel lines, their direction rotating by a small and constant angle from one plane to the other. A 180° rotation of the fibrils direction defines the half helical pitch. Superimposed series of nested arcs (see Figure 6.a for analogy) are visible on the oblique side of the model. Reprinted from Ref. 38 with permission from Elsevier.

These SEM investigations give undoubtedly evidence for the transfer of the organization of the mesophase onto the structure of the network; the standing first result of forming a polymer network into the LC solvent is the transfer of the mesophase characteristics to the polymer network during the *in situ* polymerization [26]. However, it is not possible from these pictures to give quantitative information about the size of the pores in which the LC component of the gel was located. Indeed, when the LC is extracted, the polymer network collapses to some extent in the direction perpendicular to the substrates, like it was described in previous studies on polymer-stabilized LCs [26], and, furthermore, there is some residual LC around the network fibrils.

4. Discussion

4.1. The case of *Plusiotis Resplendens* and related systems

As mentioned during the analysis of the arced patterns observed in the polymer morphology, the cholesteric structure is very frequent in different biological systems and at various scales. For example, the cuticle of many beetles exhibit optical properties such as the selective reflection of the light, and the high optical rotation of transmitted light, due to the helical structure of chitin molecules [27-29]. The rule of polarization-selectivity is also respected, apart from *Plusiotis Resplendens*: for this gold beetle, the reflected light consists of both left and right circular polarizations [29]; a half-wave plate is included in the multi-layer structure of the cuticle and functions for the wavelengths between 520 and 640 nm. Indeed, by placing two similar filters either side a $\lambda/2$ plate, the right-handed polarized light that is passed through the first filter is converted into left-handed polarized light by the $\lambda/2$ plate and reflected from the second filter. In this way a simple notch filter is produced. Man-made materials have been produced by following such a fabrication scheme. Lasing from photonic structures similar to those in the cuticle of *Plusiotis Resplendens* has been demonstrated [30]. The system comprises a dye-doped polymeric nematic defect layer sandwiched between polymeric CLC films; the reflectance in the photonic band gap region exceeds 50% due to the retardation effect and lasing occurs either at the defect mode wavelength or at the photonic band edge. Also by choosing to stack filters, it is well known that a couple of cholesteric cells with the same mean reflection wavelength but opposite helicity senses may be associated to increase the reflected light intensity [31]. The right- (left-) handed

transmitted component through the upper layer is then reflected from the layer below, passes back through the upper layer, and contributes to the reflected left- (right-) handed component from the upper layer; the total reflectance may thus approach unity. From purely practical and technological considerations, one of the goals of the solution we present here was exactly to give up the idea of stacking layers to add up their individual optical properties. Indeed, the above solutions cannot be reached with fluid media like usual low molar mass LCs or anisotropic gels (due to the diffusion between soft layers) and optical filtering with a multilayers system is sensitive to optical defects and losses at the interfaces (between organic layers or, still worse, sandwich-glass cells); additionally, it is more interesting to envisage the subsequent modification of the reflection properties by applying an electric field to a single glass cell. The increase of the reflectance is here solely obtained by playing with the thermal history of a single mixture layer during the UV-induced fabrication of the gel.

4.2. On the gel structure

The gel property which consists in exceeding the reflectance limit is attributed to the cholesteric LC being divided into two distinct environments: bulk-like material and strongly network-dominated regions [32]; LC molecules are also incorporated within the polymer strands but areas with helical states which participate to the reflection cannot be expected on such scales smaller than the pitch or even comparable to it. For the regions the furthest from the polymer strands the enclosed LC behaves bulk-like at 60°C, leading to cholesteric structures with a left-handed sense. At the closest neighbouring of polymer strands, LC material is strongly dominated by elastic

interactions with the polymer network, which templates the cholesteric order when the polymerization occurs at 112°C (when the helix sense was right-handed). The key function of these surface networks is thus to provide a thermally-stable internal memory of helicity sense. The introduction of memory effects by the presence of polymer network in relation with the elaboration conditions of the composite material are of paramount importance to open original research directions as well as to obtain novel properties for potential applications. In the case of cholesteric gels subjected to an electric field, the network can aid in the return of the initial LC director orientation and reduce the switching time for polymerization in the Grandjean texture [33]. For nematic gels cured in the nematic phase, a paranematic order in the LC in the isotropic phase induced by the network surfaces was evidenced [34]. The fact of increasing the temperature range for the properties is relevant for the operating conditions of devices [35]. Polymer-stabilized CLCs have been elaborated by combining the UV-curing with a thermally-induced pitch variation [36]. Different thermal processes were studied when the curing occurred during one single temperature of a continuous ramp for different times; in relation with the pitch variation of the blend, the reflection bandwidth can be broadened by keeping constant the band position inside the spectrum.

On the respective localization of regions with a bulk-like or network-dominated behaviour: a distribution of imbricated regions has to be emphasized, to whom a gradient of polymer network from the top to the bottom of the cell – due to a UV-polymerization gradient – may be associated. Indeed, in the same film, one side can be dominated by a dense network with frozen in chiral order and the other area by a sparse network that does not affect much the intrinsic cholesteric LC ordering. This possibility is liable to bring complexity to the understanding of the gel structure. Further

investigations of polymer morphology by transmission electron microscopy, for example, will help to progress about its structure.

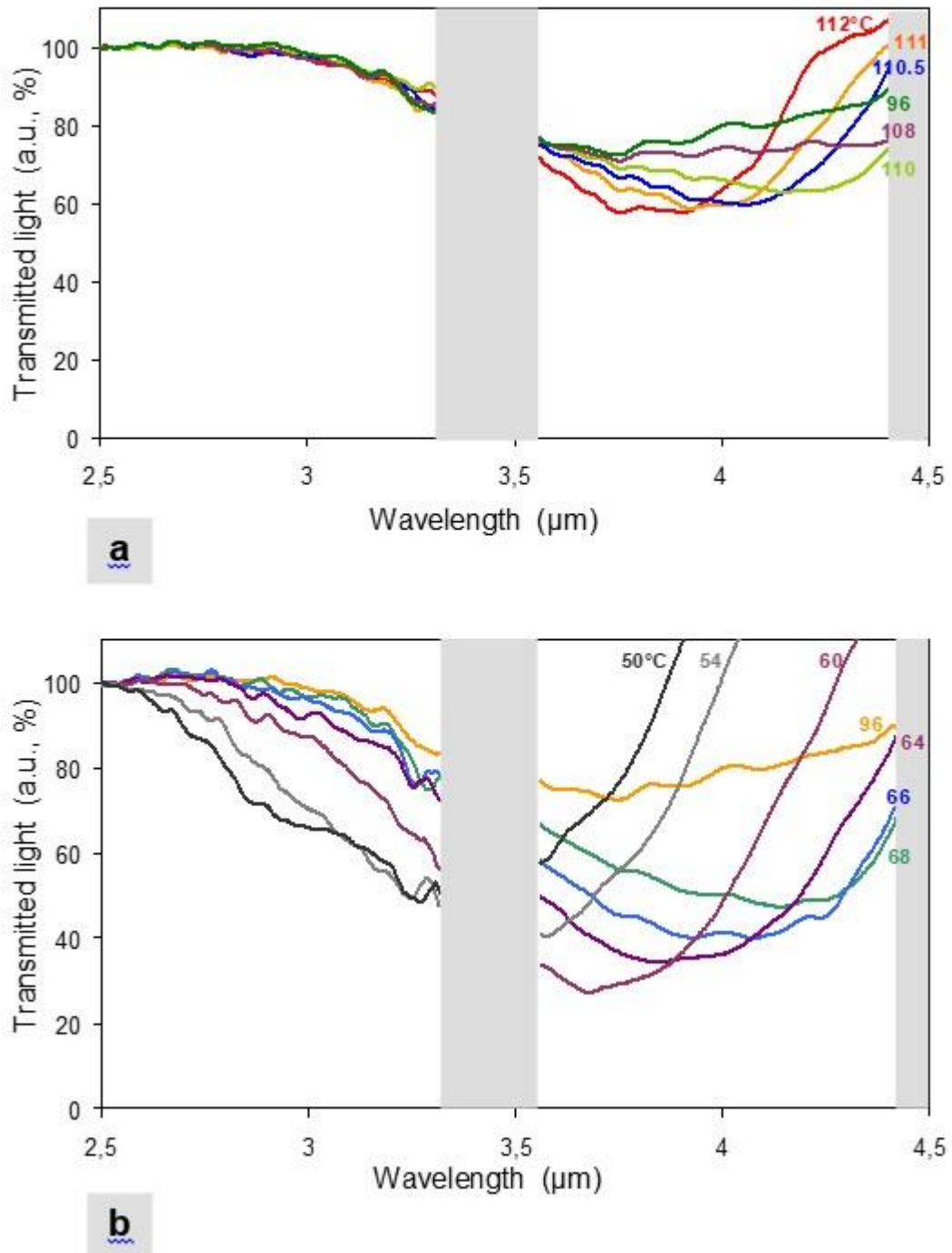


Figure 8. Normalized transmission spectra after UV-reaction when the incident light is

unpolarized and at different temperatures: above (a) and below (b) the critical temperature for the helicity inversion.

4.3. Monitoring of the optical response with the temperature

The hypothesis of a two-population system for the LC component inside the polymer network may be discussed by analyzing the behaviour of transmittance spectra with the temperature. Figure 8 shows different spectra after photoreaction at 112°C, when the temperature is changed from 112 to 96°C — close to T_c (Figure 8.a), and then up to 50°C (Figure 8.b). All the spectra at temperatures above T_c (Figure 8.a) correspond to cases for which the reflectance limit is not yet exceeded. The main position of the peak is progressively shifted towards greater wavelengths when the temperature decreases from 112 to 96°C, as a result of the pitch increase of the free fraction of the LC molecules. A quite flat peak is observed at 96°C, in the region for which the blend pitch diverges (see Figure 2): the existence of a reflection peak at this temperature is typically the signature of the twisted structure of LC molecules bound to the network which has been irreversibly formed by keeping structural characteristics of the blend mesophase at 112°C. Each peak shown in Figure 8.a is the result of the contribution of a peak assigned to the bound fraction – quite thermally stable – and a peak corresponding to the free fraction, which the position progressively changes with the temperature until it goes out of the investigation wavelength range.

Then, the spectra at temperatures below T_c (Figure 8.b) correspond to cases for which the level of reflected light intensity is being increased beyond 50%. When the temperature decreases, the peak assigned to the free population is progressively coming

back in the investigated range and, as a consequence, brings a contribution to the reflection supplementary to the one due to the structure of the bound fraction. The increased reflection is a combination of both contributions. For the spectra recorded at 60, 54 and 50°C, the amount of light transmitted for the high wavelengths exceeds 100% due to our normalisation conditions. Indeed, the spectra were normalised using the value at 2.5 μm (see sub-section 2.3), but the amount of scattered light in the gel is wavelength-dependent (it is higher for lower wavelengths [37]). This situation was not taken into account here to rescale the arbitrary units of the light intensity.

The evolution of the reflection wavelength with the temperature, as extracted from the spectra in Figure 8, is plotted in Figure 9; the reflection wavelength for the blend before curing (from Figure 2) is also reported for comparison purposes.

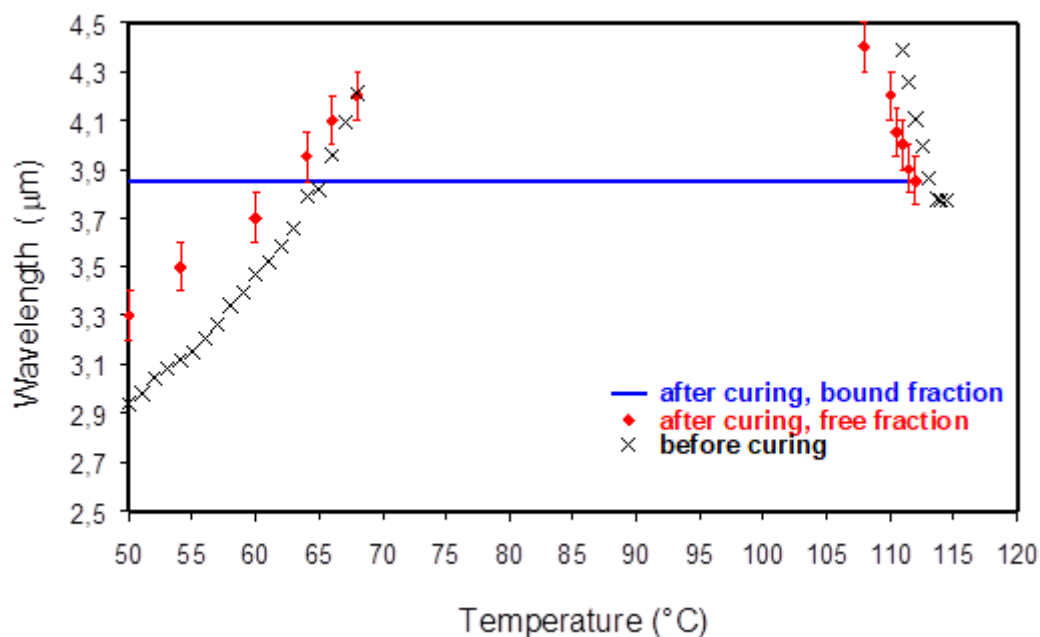


Figure 9. Variation of the reflection wavelength with the temperature after curing as extracted from Figure 8. The contributions from the free and bound fractions of LC molecules are discriminated. The data corresponding to the blend before curing are reported from Figure 2 for comparison purposes.

The mean position of the reflection peak related to the bound fraction is located just below 3.9 μm and reported like temperature-independent. The position of the peak related to the free fraction is temperature-dependent. Between 70 and 105°C the cell exhibits reflection but the related wavelength is out of the scope of the investigated range. Below 70°C, there is a slight difference between the position of the reflection peak of the blend as a function of temperature and the one associated to the free fraction. This is due to a difference in material composition; as a consequence of the phase separation, the free fraction is a part of the blend, when this last is deprived of the network-forming material, to which a small quantity of oligomers has probably to be added. The dissimilarity is reduced as soon as the temperature approaches the divergence region. The differences are minor above 100°C, for the temperatures the closest to the clarification point (to be understood as: the clarification point before curing).

The variation of the transmitted light with the temperature at 2.5 μm , *i.e.* far away from the reflection band, was also investigated. After exposure at 112°C, the amount of transmitted light is similar as before UV exposure (close to 100%). The sample is then cooled down at a controlled rate of 0.5 °C per minute. As the temperature decreases some scattering appears, giving evidence of the loss in the transmitted light amount. As the temperature changes from the clarification temperature to 100°C, the amount of transmitted light only shows a very slight decrease and remains close to 100%. But a sudden drop is observed as the critical temperature T_c is being close (*i.e.* from 100 to 85°C). This significant decrease in transmitted light is due to the very drastic changes of the helical pitch of the free fraction and associated to the surface constraints between the network and the LC molecules. It is important to notice that the slower the cooling rate

is, the smaller the transmission losses are. The LC molecules need to reorganise, a situation for which time is required; loss in transmitted light due to the scattering is enhanced when the thermal ramp is especially fast [37]. These preliminary observations are in progress and will be the scope of a forthcoming report.

5. Conclusion

Cholesteric gels with two populations of low molar mass LC molecules which are not chemically attached to the network were produced. Each population was characterized by a band of circularly polarized light which is selectively reflected. One was influenced to a large extent by the network and participated to the reflection of right-handed circularly polarized light which corresponds to the reflectivity of the material during the UV-induced network formation. The second population behaved much the same as in the bulk and participated to the reflection of left-handed circularly polarized light, which corresponds to the reflectivity of the blend at the temperature of the measurement. The association of both behaviours within a single-layer material has led to a cholesteric structure which unusually reflects more than the conventional limit of 50% of unpolarized incident light. The monitoring of the optical response with the temperature has offered the opportunity to discriminate the respective contributions of bound and free fraction of LC molecules to the reflectance and to give evidence of the progressive increase of the reflected flux when the temperature decreases from the curing temperature until the range for which both contributions of right and left circularly polarized light bands are associated.

The reflection properties were described in the infrared region – of paramount importance for regulation of temperature, telecommunications or stealthiness; however, the phenomenon is not dependent on the choice of the position for the reflection band in the spectrum. Novel opportunities to modulate the reflection over the whole light flux range, instead of only 50%, are offered; of course, the composition of the LC blend would be tuned to lower the melting point below the room temperature for application purposes. This result could open the way to the realization of CLC films with an exceptionally large flux of reflected light for smart windows in buildings and vehicles, greenhouses and other applications in which light management is desired. These are electro-optical glazing structures – made with a cholesteric film sandwiched between glass panels – having reflective and transparent modes of operation which are electrically-switchable for use in dynamically controlling electromagnetic radiation. We can also foresee reflective (polarizer-free) displays more brilliant, with a larger range of reflectivity levels.

References

- [1] de Gennes, P.-G., and Prost, J., 1993, *The Physics of Liquid Crystals*, 264-268 (Oxford: Oxford University Press).
- [2] Mitov, M., and Dessaud, N., 2006, *Nature Materials*, **5**, 361-364.
- [3] Kuball, H.-G. and Höfer, T., 2001, From a Chiral Molecule to a Chiral Anisotropic Phase. In *Chirality in Liquid Crystals*, edited by H.-S. Kitzerow and C. Bahr (New-York: Springer-Verlag), pp. 86-88.
- [4] Huff, B. P., Krich, J. J. and Collings, 2000, P. J., *Phys. Rev. E*, **61**, 5, 5372-5378.

- [5] Slaney, A. J., Nishiyama, I., Styring, P. and Goodby, J. W., 1992, *J. Mater. Chem.*, **2**, 8, 805-810.
- [6] Styring, P., Vuijk, J. D., Slaney, A. J. and Goodby, J. W., 1993, *J. Mater. Chem.* **3**, 4, 399-405.
- [7] Stegemeyer, H., Siemensmeyer, K., Sucrow, W. and Appel, 1989, *Z. Naturforsch. A* **44A**, 11, 1127-1130.
- [8] Dierking, I. *et al.*, 1993, *Liq. Cryst.*, **13**, 1, 45-55.
- [9] Kuball, H.-G., Muller, T. and Weyland, H.-G., 1992, *Mol. Cryst. Liq. Cryst.*, **215**, 271-278.
- [10] Kuball, H.-G., Muller, T., Bruning, H. and Schonhofer, A., 1995, *Mol. Cryst. Liq. Cryst.*, **261**, 845-856.
- [11] Dierking, I. *et al.*, 1994, *Z. Naturforsch.*, **49**, 1081-1086.
- [12] Dierking, I. *et al.*, 1995, *Liq. Cryst.*, **18**, 443-449.
- [13] Bahadur, B. ed., 1990, *Liquid Crystals: Applications and Uses*, Vol. 1-3 (Singapore: World Scientific).
- [14] Heppke, G., Löttsch, D. and Oestreicher, F., 1987, *Z. Naturforsch.*, **42a**, 279-283.
- [15] Broer, D. J., and Heynderickx, I., 1990, *Macromol.*, **23**, 2474-2477.
- [16] Dierking, I., Kosbar, L. L., Afzali-Ardakani, A., Lowe, A. C. and Held, G. A., 1997, *Appl. Phys. Lett.*, **71**, 17, 2454-2456.
- [17] Bouligand, Y., 1978, *Solid State Physics*, **14**, 259-294
- [18] Besseau, L. & Bouligand, Y., 1998, *Tissue & Cell*, **30**, 2, 251-260.
- [19] Neville, A. C., 1993, *Biology of Fibrous Composites: Development Beyond the Cell* (Cambridge: Cambridge University Press).
- [20] Bouligand, Y., 1972, *Tissue Cell*, **4**, 189-217.

- [21] Giraud-Guille, M.-M., 1988, *Calcif. Tissue Int.*, **42**, 167-180.
- [22] Reis, D., Vian, B. and Roland, J.-C., 1994, *Micron*, **25**, 171-187.
- [23] Livolant, F. and Leforestier, A., 1996, *Prog. Polym. Sci.*, **21**, 1115-1164.
- [24] Dierking, I., Kosbar, L. L., Afzali-Ardakani, A., Lowe, A. C. and Held, G. A., 1997, *J. Appl. Phys.*, **81**, 7, 3007-3014.
- [25] Bouligand, Y., 1965, *C. R. Acad. Sci. Paris*, **261**, 2665-3668.
- [26] Yang, D.-K., Chien L.-C. and Fung Y. K., 1996, Polymer-Stabilized Cholesteric Textures. In *Liquid Crystals in Complex Geometries*, edited by G. P. Crawford and S. Zumer (London: Taylor & Francis), pp.103-142.
- [27] Neville, A. C., 1967, *Biol. Rev.*, **42**, 421-441.
- [28] Neville, A. C. and Caveney, S., 1969, *Biol. Rev.*, **44**, 531-562.
- [29] Caveney, S., 1971, *Proc. Roy. Soc. Lond. B*, **178**, 205-225.
- [30] (a) Song, M. H. *et al.*, 2004, *Adv. Mater.*, **16**, 9-10, 779-783. (b) *ibid.*, 2004, *Sci. and Tech. of Adv. Mater.*, **5**, 437-444.
- [31] Makow, D. M., 1980, *Appl. Optics*, **19**, 8, 1274-1277.
- [32] Hikmet, R. A. M, 1991, *Mol. Cryst. Liq. Cryst.*, **198**, 357-370.
- [33] Behrens, U. and Kitzerow, H.-S., 1994, *Polym. Adv. Technol.*, **5**, 433-437.
- [34] Zumer S. and Crawford G. P., 1996, Polymer Network Assemblies in Nematic Liquid Crystals. In *Liquid Crystals in Complex Geometries*, edited by G. P. Crawford and S. Zumer (London: Taylor and Francis).
- [35] Kikuchi, H., Yokota, M., Hisakado, Y., Yang, H. and Kajiyama, T., 2002, *Nature Materials*, **1**, 64-68.
- [36] Mitov, M., Nouvet, E. and Dessaud, N., 2004, *Eur. Phys. J. E*, **15**, 413-419.
- [37] Mitov, M., and Dessaud, N., unpublished results.

[38] Besseau, L. and Giraud-Guille, M.-M., 1995, *J. Mol. Biol.* , **251**, 197-202.

Acknowledgements

We acknowledge Dr. S. Rauch, Dr. D. Loetzsch, Prof. G. Heppke and Ms. M. Dzionara (from Stranski-Laboratorium für Physikalische und Theoretische Chemie in Technische Universität Berlin) who participated to the synthesis of the helicity-inversion chiral dopant DL6 and provided us with it. C. Bourgerette (from CEMES) participated to the material preparation for SEM-FEG investigations and, with S. Leblond du Plouy (from University Paul-Sabatier, Toulouse), helped us during the observations.